

****Volume Title****

*ASP Conference Series, Vol. **Volume Number***

****Author****

© ****Copyright Year**** *Astronomical Society of the Pacific*

The Distribution of Disk-Halo HI Clouds in the Inner Milky Way

H. Alyson Ford^{1,2,3}, Felix J. Lockman⁴, and N. M. McClure-Griffiths²

¹*Centre for Astrophysics and Supercomputing, Swinburne University of Technology, Hawthorn, Victoria 3122, Australia;*

²*Australia Telescope National Facility, CSIRO Astronomy & Space Science, Epping, NSW 1710, Australia;*

³*Department of Astronomy, University of Michigan, Ann Arbor, MI 48109, USA; haford@umich.edu*

⁴*National Radio Astronomy Observatory, Green Bank, WV 24944, USA.*

Abstract. Using data from the Galactic All-Sky Survey, we have compared the properties and distribution of HI clouds in the disk-halo transition at the tangent points in mirror-symmetric regions of the first quadrant (QI) and fourth quadrant (QIV) of the Milky Way. Individual clouds are found to have identical properties in the two quadrants. However, there are 3 times as many clouds in QI as in QIV, their scale height is twice as large, and their radial distribution is more uniform. We attribute these major asymmetries to the formation of the clouds in the spiral arms of the Galaxy, and suggest that the clouds are related to star formation in the form of gas that has been lifted from the disk by superbubbles and stellar feedback, and fragments of shells that are falling back to the plane.

1. Introduction

Early observations of the disk-halo interface hinted at the presence of a handful of HI clouds connected to the Galactic disk (Prata 1964; Simonson 1971; Lockman 1984). With higher resolution data it became evident that there is a population of discrete HI clouds within this transition zone of the inner Galaxy, having sizes ~ 30 pc, masses $\sim 50 M_{\odot}$, and whose kinematics are dominated by Galactic rotation (Lockman 2002). The presence of these clouds is a widespread phenomenon; they have also been detected in the disk (Stil et al. 2006) and outer Galaxy (Stanimirović et al. 2006; Dedes & Kalberla 2010). These clouds may constitute the HI layer, and may be detected in external galaxies once resolution requirements can be met. Possible origin scenarios include galactic fountains (Shapiro & Field 1976; Bregman 1980; Houck & Bregman 1990; Spitoni, Recchi, & Matteucci 2008), superbubbles (McClure-Griffiths et al. 2006), and interstellar turbulence (Audit & Hennebelle 2005).

An analysis of the HI disk-halo cloud population in the fourth Galactic quadrant of longitude (QIV) was performed by Ford et al. (2008). To study the variation of cloud properties and distributions with location in the Galaxy, Ford, Lockman, & McClure-Griffiths (2010; hereafter FLMG) analyzed a region in the first quadrant (QI) that is mirror-symmetric about longitude zero to the QIV region, and performed an in-depth compar-

ison of the uniformly selected QI and QIV samples. In this proceeding we summarize some of the main results from that QI–QIV analysis. For an extended and complete discussion of these results we refer the reader to FLMG.

2. Observations

Disk-halo clouds were detected using data from the Galactic All-Sky Survey (GASS; McClure-Griffiths et al. 2009), which were taken with the 21 cm Multibeam receiver at the Parkes Radio Telescope. GASS is a Nyquist-sampled survey of Milky Way HI emission ($-400 \leq V_{\text{LSR}} \leq +500 \text{ km s}^{-1}$), covering the entire sky south of $\delta \leq 1^\circ$. The spatial resolution of GASS is $16'$, spectral resolution is 0.82 km s^{-1} , and sensitivity is 57 mK . The data analyzed here are from an early release of the survey which has not been corrected for stray radiation. The QI and QIV regions are mirror-symmetric about the Sun–Galactic centre line, where the QI region spans $16.9^\circ \leq \ell \leq 35.3^\circ$ and the QIV region spans $324.7^\circ \leq \ell \leq 343.1^\circ$. Both are restricted to $|b| \lesssim 20^\circ$.

3. The Tangent Point Sample

Tangent points within the inner Galaxy occur where a line of sight passes closest to the Galactic centre. This is where the maximum permitted velocity occurs assuming pure Galactic rotation, and this velocity is the terminal velocity, V_t . Random motions may push a cloud’s V_{LSR} beyond V_t , and the difference between the cloud’s V_{LSR} and V_t is defined as the deviation velocity, $V_{\text{dev}} \equiv V_{\text{LSR}} - V_t$. We define the tangent point sample of clouds as those with $V_{\text{dev}} \gtrsim 0 \text{ km s}^{-1}$ in QI and $V_{\text{dev}} \lesssim 0 \text{ km s}^{-1}$ in QIV, which results in a sample of clouds whose distances and hence physical properties can be determined. We define V_t based on observational determinations by McClure-Griffiths & Dickey (in preparation), Clemens (1985), McClure-Griffiths & Dickey (2007), and Luna et al. (2006).

4. Properties of Individual Disk-Halo Clouds

We detect 255 disk-halo HI clouds at tangent points within QI, but only 81 within QIV. A summary of the properties of the clouds within both regions is presented in Table 1, where T_{pk} is peak brightness temperature, Δv is FWHM of the velocity profile, N_{HI} is HI column density, r is radius, M_{HI} is HI mass, and $|z|$ is vertical distance from the midplane. While there are more than three times as many clouds detected in QI than in QIV, the properties of both samples are quite similar, suggesting that the clouds in both quadrants belong to the same population of clouds.

Table 1. Median Properties of Tangent Point Disk-Halo Clouds

	T_{pk} [K]	Δv [km s $^{-1}$]	N_{HI} [cm $^{-2}$]	r [pc]	M_{HI} [M_\odot]	$ z $ [pc]
QI	0.5	10.6	1.0×10^{19}	28	700	660
QIV	0.5	10.6	1.0×10^{19}	32	630	560

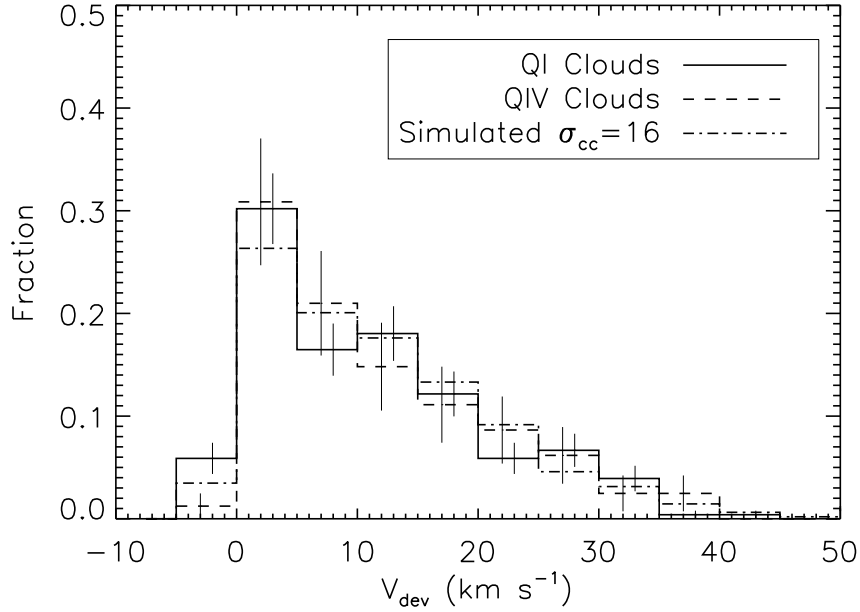


Figure 1. Distribution of observed V_{dev} for QI clouds (solid line), observed $-V_{\text{dev}}$ for QIV clouds (dashed line), and simulated V_{dev} for a population of clouds with $\sigma_{cc} = 16 \text{ km s}^{-1}$ (dash-dotted line). The QI and QIV distributions are consistent with the $\sigma_{cc} = 16 \text{ km s}^{-1}$ distribution.

5. Properties of the Disk-Halo Cloud Population

5.1. Cloud–Cloud Velocity Dispersion

Random motions, characterized by a cloud–cloud velocity dispersion (σ_{cc}), can increase the V_{LSR} of a cloud that is located near a tangent point to values beyond V_t . We can determine the magnitude of these random motions based on the deviation velocity distribution of the tangent point cloud samples. The observed V_{dev} distributions are presented in Figure 1. The steep decline towards larger V_{dev} shows that the clouds’ motions are governed by Galactic rotation. The distributions have a K-S probability of 76% of being drawn from the same population, suggesting the QI and QIV clouds have identical σ_{cc} . Both populations have distributions consistent with those of simulated populations that have a random velocity component derived from a Gaussian with dispersion $\sigma_{cc} = 16 \text{ km s}^{-1}$.

5.2. Vertical Distribution

More clouds are detected at most heights within QI than QIV, as can be seen from their observed vertical distributions (Figure 2). The decrease in the number of clouds at low $|z|$ is due to confusion, as it is increasingly difficult to detect clouds at lower $|z|$ and lower $|V_{\text{dev}}|$. The vertical distribution of clouds in QI is best represented by an exponential with $h = 800 \text{ pc}$, while in QIV the scale height is only $h = 400 \text{ pc}$. These values are not in agreement, and as σ_{cc} is similar in both quadrants, the scale height of the clouds

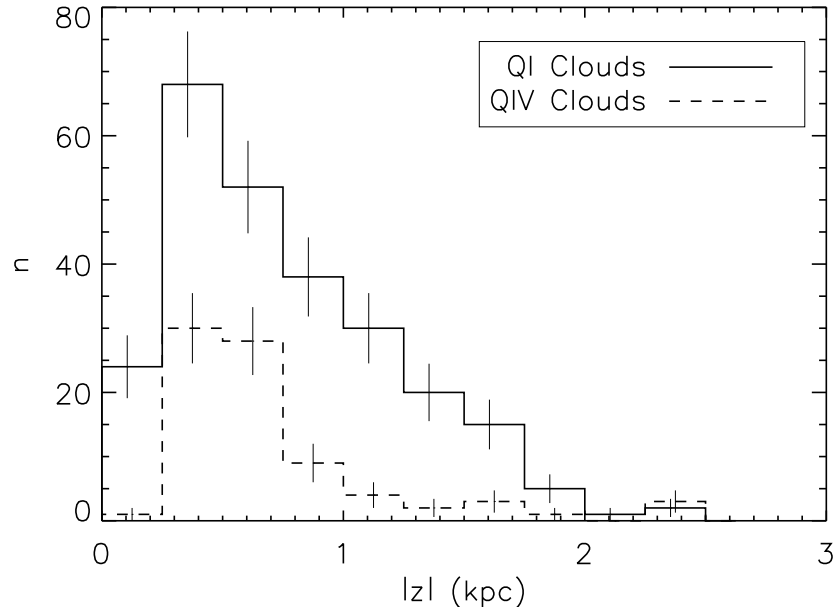


Figure 2. Distribution of observed $|z|$ for the QI (solid line) and QIV (dashed line) clouds. There are significantly more clouds at most $|z|$ in QI than QIV and the scale height is twice as large.

is not linked to the cloud–cloud velocity dispersion; even if $\sigma_{cc} = \sigma_z$, this would only propel clouds to $h < 100$ pc within the mass model of Kalberla et al. (2007).

5.3. Longitude Distribution

The observed longitude distributions of clouds in the QI and QIV regions are shown in Figure 3. Not only are there more clouds at all $|\ell|$ in the QI region, but they are more uniformly distributed compared to the peaked QIV distribution at $\ell \sim 25^\circ$. The radial distribution is directly related to the longitude distribution; $R \equiv R_0 \sin \ell$ at the tangent point, where R_0 is the radius of the solar circle. The radial distribution of the QI sample is also more uniform compared to QIV, where instead the distribution peaks and declines rapidly at $R > 4.2$ kpc.

6. Implications for the Disk-Halo Clouds

While the cloud–cloud velocity dispersions in both quadrants are consistent, the number of clouds detected, along with the vertical and radial distributions, differ dramatically. We have searched for possible systematic effects that might account for the asymmetry but have found none of any significance. These asymmetries imply that the clouds are linked to Galactic structure and events occurring in the disk. We have overlaid the QI and QIV regions on what we believe to be the most appropriate representation of the large-scale Galactic structure to date, which includes recent results from the Galactic

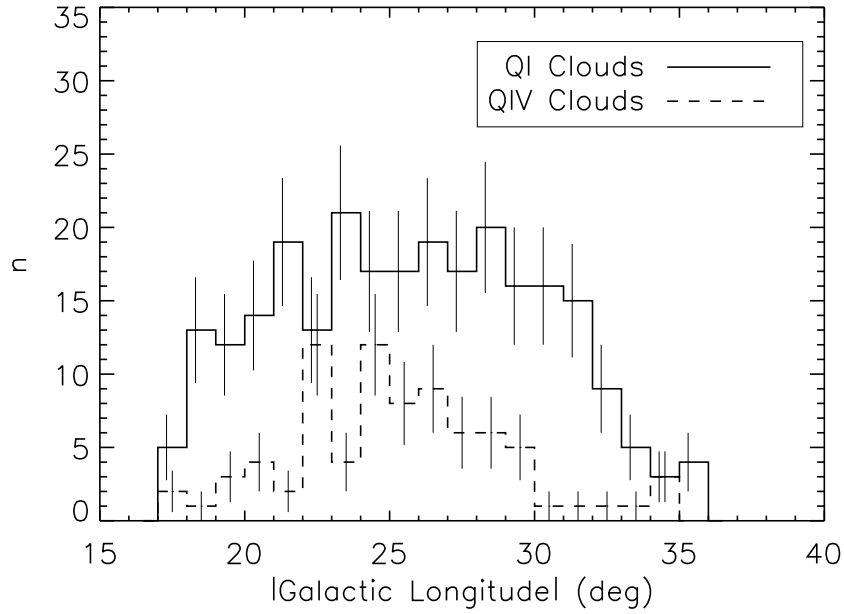


Figure 3. Observed longitude distributions of the QI (solid line) and QIV (dashed line) regions. More clouds are seen in QI at all ℓ than in QIV. The distribution is more uniform in QI while it is peaked around $\ell \sim 25^\circ$ in QIV.

Legacy Infrared Mid-Plane Survey Extraordinaire (GLIMPSE; Benjamin et al. 2003) on the location of the bar and spiral arms (Benjamin et al. 2005; see Figure 4). The solid lines enclose the QI and QIV regions, with a line of sight extent equivalent to $\sim 1\sigma_{cc}$ volume around the tangent point. A striking asymmetry within the Galaxy that is immediately apparent is that the QIV region contains only a minor arm while the QI region contains the merging of the near-end of the bar and a major spiral arm.

The distribution of disk-halo clouds mirrors the spiral structure of the Milky Way, suggesting a correlation with star formation. The spatial relation between extraplanar gas to star formation activity in some external galaxies further supports this hypothesis (Barbieri et al. 2005). More clouds occur in a region of the Galaxy including the near-end of the bar and a major spiral arm, while there are fewer clouds in a region including only a minor arm. The number of clouds likely correlates with the level of star formation activity, and the different scale heights may represent different evolutionary stages or varying levels of star formation. The clouds are likely formed by gas that is lifted by superbubbles and stellar feedback, and some may result from fragmenting supershells. Supershells have much larger timescales than star-forming regions (~ 20 – 30 Myr versus ~ 0.1 Myr; de Avillez & Breitschwerdt 2004; McClure-Griffiths et al. 2006; Prescott et al. 2007), and so clouds may not be near regions of current star formation. If clouds are lifted by events within the disk, large cloud–cloud velocity dispersions are not required to produce the derived scale heights of the disk-halo clouds.

Disk-halo clouds are abundant within the Milky Way, and it is likely that many clouds would be detected at other longitudes corresponding with spiral features.

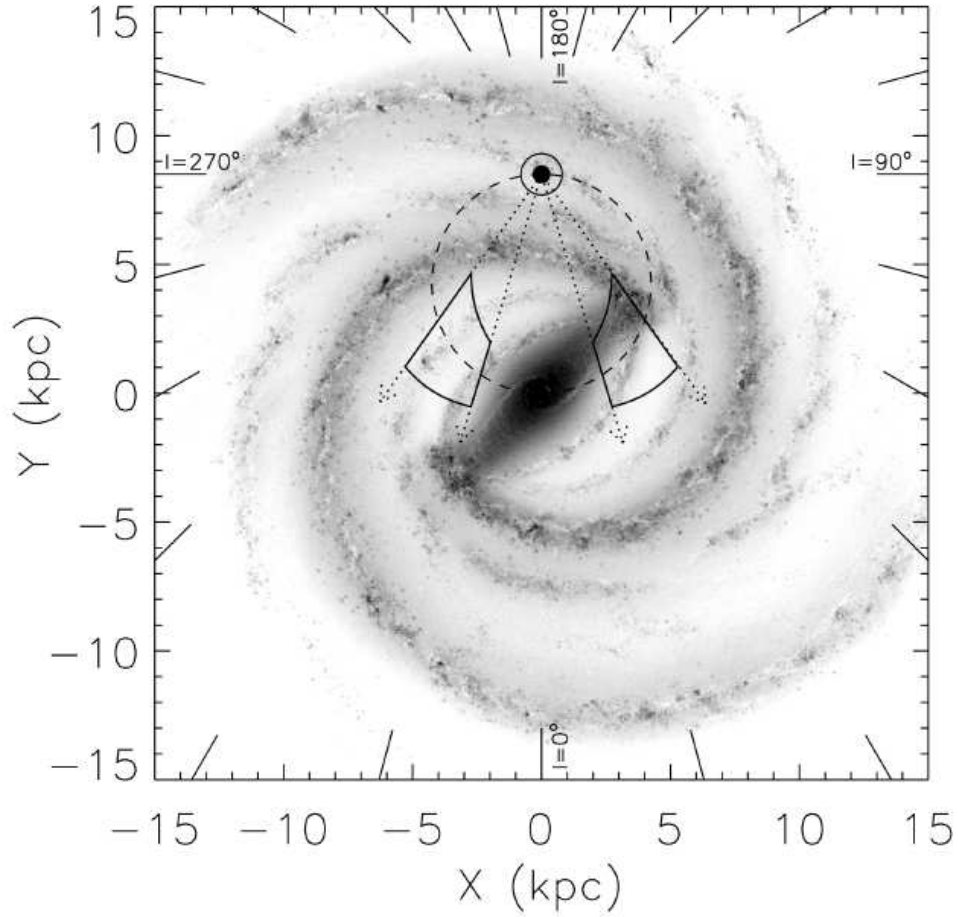


Figure 4. Figure from FLMG showing an artist's conception of the Milky Way. The solid lines enclose the QI and QIV regions, where QI covers the region where the near-end of the Galactic bar merges with a major spiral arm and QIV covers only a minor arm. The artist's conception image is from NASA/JPL-Caltech/R. Hurt (SSC-Caltech).

Acknowledgments. We thank B. Saxton for his help creating Figure 4. HAF thanks the National Radio Astronomy Observatory for support under its Graduate Student Internship Program. The National Radio Astronomy Observatory is operated by Associated Universities, Inc., under a cooperative agreement with the National Science Foundation. The Parkes Radio Telescope is part of the Australia Telescope which is funded by the Commonwealth of Australia for operation as a National Facility managed by CSIRO.

References

- Audit, E., & Hennebelle, P. 2005, *A&A*, 433, 1
- Barbieri, C. V., Fraternali, F., Oosterloo, T., Bertin, G., Boomsma, R., & Sancisi, R. 2005, *A&A*, 439, 947
- Benjamin, R. A., Churchwell, E., Babler, B. L., Bania, T. M., Clemens, D. P., Cohen, M., Dickey, J. M., Indebetouw, R., Jackson, J. M., Kobulnicky, H. A., Lazarian, A., Marston, A. P., Mathis, J. S., Meade, M. R., Seager, S., Stolovy, S. R., Watson, C., Whitney, B. A., Wolff, M. J., & Wolfire, M. G. 2003, *PASP*, 115, 953
- Benjamin, R. A., Churchwell, E., Babler, B. L., Indebetouw, R., Meade, M. R., Whitney, B. A., Watson, C., Wolfire, M. G., Wolff, M. J., Ignace, R., Bania, T. M., Bracker, S., Clemens, D. P., Chomiuk, L., Cohen, M., Dickey, J. M., Jackson, J. M., Kobulnicky, H. A., Mercer, E. P., Mathis, J. S., Stolovy, S. R., & Uzen, B. 2005, *ApJ*, 630, L149
- Bregman, J. N. 1980, *ApJ*, 236, 577
- Clemens, D. P. 1985, *ApJ*, 295, 422
- de Avillez, M. A., & Breitschwerdt, D. 2004, *A&A*, 425, 899
- Dedes, L., & Kalberla, P. W. M. 2010, *A&A*, 509, 60
- Ford, H. A., Lockman, F. J., & McClure-Griffiths, N. M. 2010, *ApJ*, 722, 367
- Ford, H. A., McClure-Griffiths, N. M., Lockman, F. J., Bailin, J., Calabretta, M. R., Kalberla, P. M. W., Murphy, T., & Pisano, D. J. 2008, *ApJ*, 688, 290
- Houck, J. C., & Bregman, J. N. 1990, *ApJ*, 352, 506
- Kalberla, P. M. W., Dedes, L., Kerp, J., & Haud, U. 2007, *A&A*, 469, 511
- Lockman, F. J. 1984, *ApJ*, 283, 90
- 2002, *ApJ*, 580, L47
- Luna, A., Bronfman, L., Carrasco, L., & May, J. 2006, *ApJ*, 641, 938
- McClure-Griffiths, N. M., & Dickey, J. M. 2007, *ApJ*, 671, 427
- McClure-Griffiths, N. M., Ford, A., Pisano, D. J., Gibson, B. K., Staveley-Smith, L., Calabretta, M. R., Dedes, L., & Kalberla, P. M. W. 2006, *ApJ*, 638, 196
- McClure-Griffiths, N. M., Pisano, D. J., Calabretta, M. R., Ford, H. A., Lockman, F. J., Staveley-Smith, L., Kalberla, P. M. W., Bailin, J., Dedes, L., Janowiecki, S., Gibson, B. K., Murphy, T., Nakanishi, H., & Newton-McGee, K. 2009, *ApJS*, 181, 398
- Prata, S. W. 1964, *Bull. Astron. Inst. Netherlands*, 17, 511
- Prescott, M. K. M., Kennicutt, R. C., Jr., Bendo, G. J., Buckalew, B. A., Calzetti, D., Engelbracht, C. W., Gordon, K. D., Hollenbach, D. J., Lee, J. C., Moustakas, J., Dale, D. A., Helou, G., Jarrett, T. H., Murphy, E. J., Smith, J., Akiyama, S., & Sosey, M. L. 2007, *ApJ*, 668, 182
- Shapiro, P. R., & Field, G. B. 1976, *ApJ*, 205, 762
- Simonson, S. C., III 1971, *A&A*, 12, 136
- Spitoni, E., Recchi, S., & Matteucci, F. 2008, *A&A*, 484, 743
- Stanimirović, S., Putman, M., Heiles, C., Peek, J. E. G., Goldsmith, P. F., Koo, B.-C., Krčo, M., Lee, J.-J., Mock, J., Muller, E., Pandian, J. D., Parsons, A., Tang, Y., & Werthimer, D. 2006, *ApJ*, 653, 1210
- Stil, J. M., Lockman, F. J., Taylor, A. R., Dickey, J. M., Kavars, D. W., Martin, P. G., Rothwell, T. A., Boothroyd, A. I., & McClure-Griffiths, N. M. 2006, *ApJ*, 637, 366